Journal of the Korean Nuclear Society
Volume 29, Number 6, pp468~475, December 1997

Transient Photocurrent in Amorphous Silicon Radiation Detectors

Hyoung-Koo Lee, Tae-Suk Suh, Bo-Young Choe, and Kyung-Sub Shinn
Catholic University of Korea
505 Banpo-Dong, Seocho-Gu, Seoul, 137-040 Korea

Gyu-Seong Cho
Korea Advanced Institute of Science and Technology
373-1 Kusong-Dong, yusong-Gu, TaeJun, 305-701 Korea

(Received June 17, 1997)

Abstract

The transient photocurrent in amorphous silicon radiation detectors (n-i-n and forward biased p-i-n) were analyzed. The transient photocurrents in these devices could be modeled using multiple trap levels in the forbidden gap. Using this model the rise and decay shapes of the photocurrents could be fitted. The decaying photocurrent shapes of the p-i-n and n-i-n devices after a short duration of light pulse showed a similar behavior at low dark current density levels, but at higher dark current density levels the photocurrent of the p-i-n diode decayed faster than that of the n-i-n, which could be explained by the decreased electron lifetimes in the forward biased p-i-n diode at high dark current densities. The transient photoconductive gain behaviors in the amorphous silicon radiation detectors are discussed in terms of device configuration, dark current density and time scale.

1. Introduction

Amorphous silicon (a-Si:H) has been investigated as the material for radiation detection and has shown the ability of detecting visible light, x-rays, gamma-rays, charged particles and neutrons.[1-4] As it is possible to fabricate the amorphous silicon radiation detectors in pixel format on a large area substrate, many efforts have been made to produce large area radiation imaging devices based on the two-dimensional amorphous silicon radiation detector arrays.[2,5,6] The p-i-n configuration has been conventionally used as the structure of the amorphous silicon radiation detectors, and the basic principle involved in radiation detection technique is to measure the signal which is induced by the motion of the charge carriers along the depletion field in the i-region of the reverse biased p-i-n diode. In this case, the maximum value of the photoconductive gain which is defined as the ratio of the collected charge to the number of interacted photons is unity, that is, the amount of the collected charge cannot exceed the amount of the photo-induced

charge. By utilization of the photoconductive gain mechanism, however, the signal size can be increased. The photoconductive gain is usually utilized in the steady state, and for normal a-Si:H it takes hundreds of microseconds or a few milliseconds to achieve steady state photoconductive gain. For radiation detection using a-Si:H, a scintillator layer such as CsI(Tl) is usually coupled to a-Si:H devices to convert the radiation to visible light. As the fluorescence decay time of CsI(Tl) is about 1 μsec, the duration of light exposure is about 1 μsec for a fast transit charged particle or a gamma-ray, and a few milliseconds for an x-ray exposure in medical imaging. Therefore during the short duration of light exposure from CsI(Tl) in radiation detection, the full photoconductive gain cannot be achieved. If, however, a moderate gain can be obtained during a short period of time, this photoconductive gain mechanism may be utilized in radiation detection using a-Si:H devices. Experimental results of the photoconductive gain in a-Si:H p-i-n, n-i-n and n-i-p-i-n devices in connection with radiation detection were previously reported, and gains of 3 ~9 for short pulses of radiation (<1 μsec) and gains of more than 200 for longer pulses (≥ 1 msec) could be achieved.[7] In Fig. 1, experimentally obtained photoconductive gains of the n-i-n and forward biased p-i-n devices for 1 msec of light pulses are shown. In this paper, we discuss the transient behavior of the photocurrent in a-Si:H n-i-n and forward biased p-i-n devices so that we can understand the similarities and differences of the transient photoconductive gain mechanisms in each type of the devices.

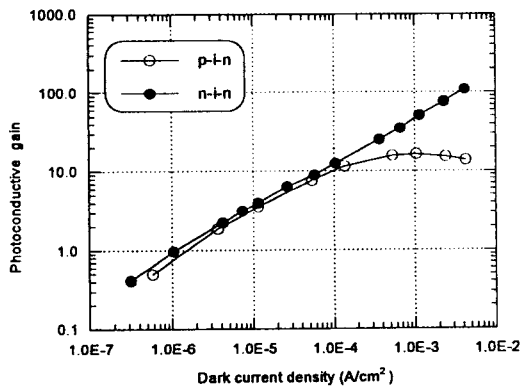

Fig. 1. Comparisons of the Photoconductive Gains in p-i-n Photodiodes and n-i-n Photo-Conductors. The Thickness of the Devices is 14 μm and 1 msec of Light was Exposed.

2. Theory

2.1. Primary Photocurrent and Secondary Photocurrent

There are two types of photosensitive devices made of insulating or semiconducting materials: photoconductors and photodiodes. The typical structures of these devices are schematically shown in Fig. 2 (a) and (b). Usually, photodiodes have a sandwich structure, and photoconductors have a gap geometry with coplanar electrodes as shown in the figure, but, sometimes, sandwich structured photoconductors are also made. The basic difference in these two devices is the type of the contacts. The contacts in the photoconductors are ohmic, while photodiodes have blocking contacts when those are reverse biased. Due to this difference in the contact type, both the dark current and the photocurrent behaviors in

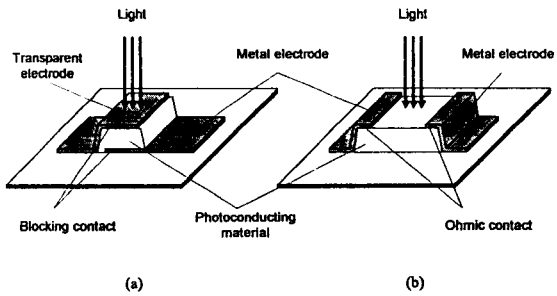

Fig. 2. Typical Structures of (a) Photodiode and (b) Photoconductor. The Contacts of a Photodiode are Blocking in Reverse Bias While Those of a Photoconductor are Ohmic.

photoconductors and reverse biased photodiodes are quite different.

A blocking contact prevents injection of charge carriers through it, hence the dark current in a reverse biased photodiode is mainly due to the thermal generation current in the bulk of the device, and the maximum photocurrent is simply limited by the optical generation rate therefore the gain is limited to unity. The photocurrent in a reverse biased photodiode is termed primary photocurrent.[8,9] The flow of charge carriers in a reverse biased photodiode is shown in Fig. 3 (a). Amorphous silicon p-i-n devices are photodiodes since in reverse bias the n- and p- layer prevents injection of holes and electrons, respectively. The maximum photocurrent density of a reverse biased photodiode which is exposed to a uniform light generating F electron-hole pairs per second per unit volume is

$$J_{pri} = qFd \quad . \qquad (1)$$

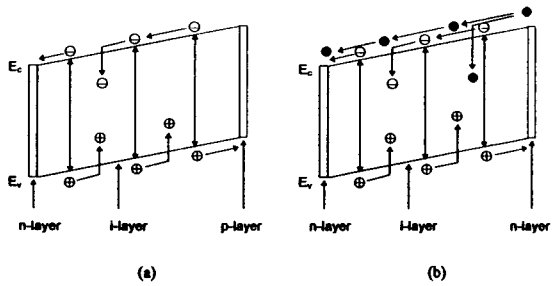

Fig. 3. Schematic Representation of Photogenerated Charge Carrier Flow in (a) Reverse Biased p-i-n Photodiode and (b) n-i-n Photoconductor. Circles with a Minus Represent Photo-Induced Electrons and Circles with a Plus Represent Photo-Induced Holes. Solid Circles in a Photoconductor Represent Injected Electrons from the Cathode. Note that in a Photodiode Free Carriers are Generated Only by Photon Interactions, While in a Photoconductor Injection of Carriers (Electrons in this Case) Enhances the Photocurrent.

where q is the charge of an electron and d is the thickness of the diode. In Eq. (1) the recombination of the charge carriers during their transit was neglected, that is, a full collection efficiency was assumed, which is a satisfying assumption when the reverse bias is sufficiently high such that the mean free path of the minority carriers is longer than the diode thickness and both the majority and minority charge carrier densities are low. The photoresponse speed of a-Si:H photodiodes is fast (less than 10 nsec) compared to that of photoconductors, but the signal is small, hence they are suitable for high speed large signal measurements.

In photoconductors or forward biased photodiodes, the contacts are ohmic, hence injection current flows when a bias is applied. Due to this injection current, the dark current in forward biased photodiodes or photoconductors is much higher than the corresponding reverse biased photodiodes. The ohmic contacts can always supply the current required by the photoconductor and this mode of photocurrent is referred to as a secondary photocurrent.[8,9] In this case, whenever a charge carrier which is induced by a photon reaches an electrode, it is replenished at the other electrode. Therefore the photocurrent keeps flowing until all the photo-induced carriers disappear by recombination. Various cases of secondary photocurrents are well described in Reference 9. The transport mechanism of the secondary photocurrent is schematically shown in Fig. 3 (b), in which single carrier (electron) injection is allowed as the device has the n-i-n configuration. Usually, photoconductors or forward biased photodiodes have a high photo-signal but slow photoresponse and high dark current, therefore their usage is usually limited to low event rate or steady state measurements of small signals. Derivations of the secondary photocurrent and the photoconductive gain in photoconductors are as follows. Consider a

photoconductor which is made of an insulator or a semiconductor with a single trap level and a single recombination level as shown in Fig. 4. Assuming electrons are the majority carriers and the contribution of hole photoconductivity is negligible, the continuity equations of electrons are

$$\frac{dn_f}{dt} = F + \frac{n_t}{\tau_{rel}} - \frac{n_f}{\tau_{tr}} - \frac{n_f}{\tau_l}$$
$$\frac{dn_t}{dt} = \frac{n_f}{\tau_{tr}} - \frac{n_t}{\tau_{rel}} \qquad (2)$$

where n_f and n_t are the free and trapped electron density, respectively, F is the optical generation rate which is assumed constant, τ_{rel} is the thermal excitation time of trapped electrons, τ_{tr} is the trapping time of free electrons in the conduction band and τ_l is the recombination lifetime of free electrons. n_f/τ_{tr} corresponds to the trapping rate of free electrons by the single trap level, and n_t/τ_{rel} is the thermal release rate of the trapped electrons from the trap. In Eq. (2), free and trapped electron densities are assumed to be spatially uniform, and the thermal generation rate from the recombination centers is neglected because the number of electrons in the conduction band is mostly determined by the injected electrons rather than the thermally generated electrons. If we assume that $\tau_{tr} \ll \tau_{rel}$ and $\tau_{tr} \ll \tau_l$, the solution of Eq. (2) is

$$n_f(t) = F\left\{\tau_l\left[1-\exp\left(-\frac{t}{\tau_{res}}\right)\right] + \tau_{tr}\left[1-\exp\left(-\frac{t}{\tau_{tr}}\right)\right]\right\} \qquad (3)$$

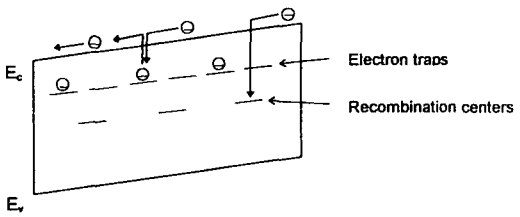

Fig. 4. Schematic Energy Band Diagram of a Photoconductor with a Single Trap Level and a Single Recombination Center Level.

where τ_{res} is the response time of the photoconductor defined as

$$\tau_{res} = \frac{\tau_{rel}}{\tau_{tr}}\tau_l \qquad (4)$$

If there are no traps the response time is equal to the recombination lifetime of electrons τ_l. If the time of interest t is much greater than τ_{tr}, Eq. (3) is reduced to

$$n_f(t) = F\tau_l\left[1-\exp\left(-\frac{t}{\tau_{res}}\right)\right] \qquad (5)$$

Using Eq. (3), the secondary photocurrent density can be derived as

$$J_{sec}(t) = \frac{qn_f(t)d}{t_r} = \frac{qFd\tau_l}{t_r}\left\{1-\exp\left(-\frac{t}{\tau_{res}}\right) + \frac{\tau_{tr}}{\tau_l}\left[1-\exp\left(-\frac{t}{\tau_{tr}}\right)\right]\right\} \qquad (6)$$

where t_r is the transit time of a free electron from one contact to another. By dividing the secondary photocurrent in Eq. (6) by the maximum primary photocurrent in Eq. (1), the photoconductive gain is expressed as

$$G(t) = G_{ss}\left\{1-\exp\left(-\frac{t}{\tau_{res}}\right) + \frac{\tau_{tr}}{\tau_l}\left[1-\exp\left(-\frac{t}{\tau_{tr}}\right)\right]\right\} \qquad (7)$$

where $G_{ss} = \tau_l/t_r$ is the well known steady state photoconductive gain which was originally derived by Rose[9,10]. In steady state the ratio of τ_{rel} to τ_{tr} is equal to n_t/n_f, hence the response time in Eq. (4)

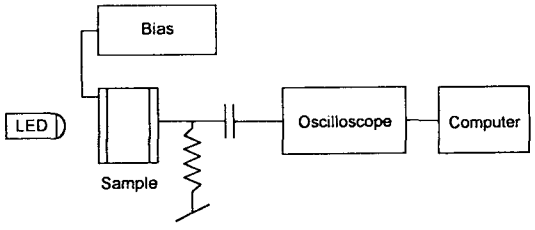

Fig. 6. Experimental System for the Measurement of Photocurrents from Amorphous Silicon p-i-n or n-i-n Device Samples. The Photocurrent was Directly Read by an Oscilloscope via ac Coupling.

can be expressed as

$$\tau_{res} = \frac{n_t}{n_f}\tau_l \quad , \tag{8}$$

which is in agreement with Rose's definition of response time.[10]

2.2 Photocurrent in a-Si:H Photoconductors

Since a-Si:H has a distribution of trap levels in the forbidden gap, simple expressions of the continuity equations as in Eq. (2) are not adequate. Assuming K levels of traps in the forbidden gap, the continuity equations for a-Si:H photoconductors are

$$\begin{aligned} \frac{dn_f}{dt} &= F + \sum_i^K \left(\frac{n_{t,i}}{\tau_{rel,i}}\right) - n_f \sum_i^K \left(\frac{1}{\tau_{tr,i}}\right) - \frac{n_f}{\tau_l} \\ \frac{dn_{t,i}}{dt} &= \frac{n_f}{\tau_{tr,i}} - \frac{n_t}{\tau_{rel,i}} \quad , \quad i = 1,2,\ldots K \end{aligned} \tag{9}$$

Of course it is not possible to solve these $K+1$ set of differential equations analytically, but from the current expression in Eq. (6), we can expect that the rise of the photocurrent in a-Si : H photoconductors may be approximated using multicomponent exponentials. The expected photocurrent density equation in a-Si:H photoconductors is

$$J_p(t) = J_{ss}\left(1 - \sum_i a_i e^{-t/\tau_i}\right) \quad , \tag{10}$$

where $J_{ss} = J_{pri}G_{ss}$ is the photocurrent density at steady state, τ_i is a response time which corresponds to the i-th trap and a_i is a weighting factor which represents the influence of the i-th trap to the photocurrent. The summation of ai is equal to 1. It is not easy to extract physically meaningful information from a_i due to the complexity of the differential equations, but we may conjecture that, based on the expression in Eq. (6), ai may be related to the trapping time to the i-th trap. By the same procedure, the decay of the photocurrent density after shutting off the light can be expressed as

$$J_p(t) = J_o \sum_i a_i e^{-t/\tau_i} \quad , \tag{11}$$

where J_o is the photocurrent density at the moment the light is shut off.

3. Experiment

Amorphous silicon p-i-n and n-i-n device samples were fabricated using PECVD(Plasma Enhanced Chemical Vapor Deposition) machine and all of the samples had a sandwich structure. The i-layer was 14μm thick and p- and n-layer were 30nm thick. These p-and n-layers provided ohmic contacts in forward bias which is essential for the photoconductive gain as discussed in Section 2.1.

The photocurrents from p-i-n or n-i-n devices were directly measured by an oscilloscope as shown in Fig. 5. Using ac coupling, the dc dark current could be separated from the photocurrent. The RC time constant of the measurement system was made long enough($>$1 sec) to prevent decay of the photocurrent level. Data of the measured photocurrent were stored in a computer which is connected to the digital oscilloscope.

4. Results and Discussion

The measured photocurrent shape in a forward biased a-Si:H p-i-n diode with 1 msec light pulse is shown in Fig. 6 with the curves fitted by Eq. (10) and (11), where a_i and τ_i were used as fitting parameters. As shown in this figure, the multicomponent exponential terms are adequate to express the rise and decay of the transient photocurrents in a-Si:H photoconductors or forward biased photodiodes.

It has been experimentally shown that the photocurrent, hence the photoconductive gain, is recombination centers broadened[8-10], therefore and (b), the measured photocurrent shapes of the a-Si:H n-i-n and forward biased p-i-n devices at

two different dark current densities are compared. At the same dark current densities, the initial decay times of the p-i-n and n-i-n devices are almost identical, therefore their photoconductive gains are almost the same for the short light pulses (order of μsec) at any dark current level. At higher dark current levels, however, the photocurrent of the p-i-n diode decays faster than that of the n-i-n device for the longer time scales as shown in Fig. 7 (b), and this causes the photoconductive gain of the forward biased p-i-n diodes to be less than that of the corresponding n-i-n photoconductor at high dark current density levels as shown in Fig. 1. This decreasing decay time constant in the forward biased p-i-n diode may be explained by the decrease of the electron lifetime. As the forward bias increases, the dark current density increases due to the increasing amount of electrons and holes by double injections from the contacts, and correspondingly the quasi-Fermi energy levels of the electrons and holes move toward the band edges since they are related to the free carrier densities as

$$E_c - E_{Fn} = kT\ln\left(\frac{N_c}{n_f}\right)$$
$$E_{Fp} - E_v = kT\ln\left(\frac{N_v}{p_f}\right) \quad , \qquad (12)$$

where E_c is the conduction band edge, E_v is the valence band edge, E_{Fn} and E_{Fp} is the quasi-Fermi energy level of electrons and holes, respectively,

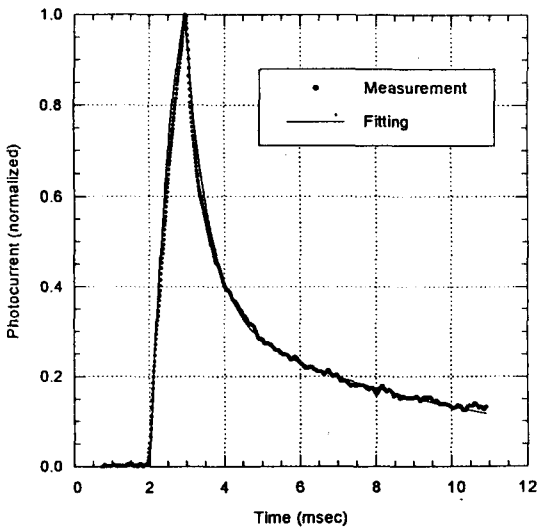

Fig. 6. Photocurrent Shape in a Forward Biased a-Si:H p-i-n Diode with 1 msec Light Pulse. The Current is Normalized to the Maximum Current at 1 msec. 3 V of Forward Bias was Applied. Eq. (10) and (11) were Used to Fit the Measurement.

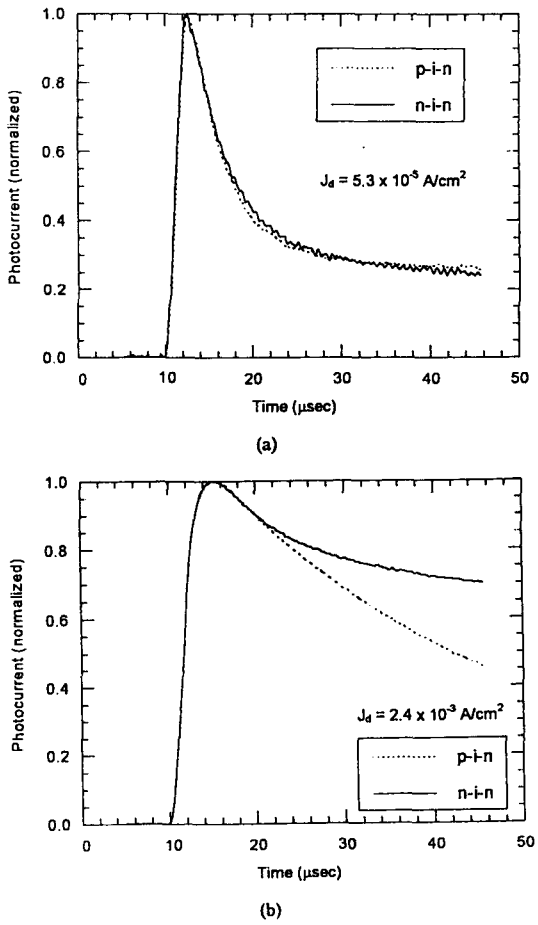

Fig. 7. The Decaying Photocurrent Shapes of n-i-n and Forward Biased p-i-n Devices After a Short Light Pulse at two Different Dark Current Levels. (a) 2.2μsec Light Pulse, 5.3×10^{-5}A/cm^{2}Dark Current Density. (b) 5μsec Light Pulse, 2.4×10^{-3}A/cm^2 Dark Current Density

N_c and N_v is the density of states at the conduction band edge and valence band edge, respectively, n_f is the free electron density and p_f is the free hole density. Accordingly, the demarcation levels also move toward the band edges making the recombination centers broadened[8-10], therefore more recombination of electrons and holes occurs and eventually the lifetime of the electrons is decreased. Due to this decrease in the electron lifetime, the photocurrent of the forward biased p-i-n diode decreases at high forward biases, since J_{ss} in Eq. (10) is proportional to the electron lifetime τ_l. At low dark current density, however, the increase of the value in the parenthesis in Eq. (10) is more dominant than the decrease in J_{ss} with the bias, therefore the photocurrent increases with the bias, hence with the dark current density as shown in Fig. 1. The decrease of the electron lifetime and the photoconductive gain with the increase of voltage in the forward biased p-i-n diodes has also been found by others[11,12].

5. Conclusions

The transient photocurrent in a-Si:H n-i-n and forward biased p-i-n devices were modeled and analyzed. As the amorphous silicon has a distribution of trap levels in the forbidden gap a simple expression from a single trap and a single recombination level model cannot fit the measurements. Using the multiple trap level model, the transient photocurrent could be expressed with multicomponents of the exponential terms and could successfully fit the measured photocurrent shapes. The decay times of the photocurrent in n-i-n and forward biased p-i-n devices were almost identical in short time scales but in the longer time scales the decay time of the photocurrent in the forward biased p-i-n diodes decreased as the dark current density was increased, which was due to the decrease of the electron lifetime. Therefore, the photoconductive gains in p-i-n and n-i-n devices are almost the same for the short light pulses (~μsec), however, n-i-n photoconductors produce higher gains than corresponding forward biased p-i-n diodes for the longer light pulses (~msec) at high dark current densities. According to this study, when one wants to make use of the photoconductive gain mechanism of a-Si:H in radiation detection, either of the n-i-n and p-i-n devices may be used for the fast radiation detection, and n-i-n photoconductor is a better choice than p-i-n photodiode when detecting radiations of a rather longer duration such as the medical x-rays.

References

1. V. Perez-Mendez, J. Morel, S. N. Kaplan, and R. A. Street, "Detection of Charged Particles in Amorphous Silicon Layers," *Nucl. Instr. And Meth. A*, **252**, 478 (1986).
2. I. Fujieda, S. Nelson, P. Nylen, R. A. Street, and R. L. Weisfield, "Two Operation Modes of 2D a-Si Sensor Arrays for Radiation Imaging," *J. Non-Cryst. Solids*, **137&138**, 1321 (1991).
3. I. Fujieda, G. Cho, J. S. Drewery, T. Gee, T. Jing, S. N. Kaplan, V. Perez-Mendez, and D. Wildermuth, "X-Ray and Charged Particle Detection with CsI(Tl) Layer Coupled to a-Si:H Photodiode Layers," *IEEE Trans. Nucl. Sci.*, **38**, 255 (1991).
4. A. Mireshghi, G. Cho, J. S. Drewery, W. S. Hong, T. Jing, H. K. Lee, S. N. Kaplan, and V. Perez-Mendez, "High Efficiency Neutron Sensitive Amorphous Silicon Pixel Detectors," *IEEE Trans. Nucl. Sci.*, **41**, 915 (1994).
5. I. Fujieda, S. Nelson, R. A. Street and R. L. Weisfield, "Radiation Imaging with 2D a-Si Sensor Arrays," *IEEE Trans. Nucl. Sci.*, **39**, 1056 (1992).

6. L. E. Antonuk, J. Yorkston, W. Huang, J. Boudry, E. J. Morton, "Large Area, Flat-Panel a-Si:H Arrays for X-Ray Imaging," *SPIE Proc.* **1896**, 18 (1993).
7. H. K. Lee, J. S. Drewery, W. S. Hong, T. Jing, S. N. Kaplan and V. Perez-Mendez, "Photoconductive Gain in Hydrogenated Amorphous Silicon Devices And Its Applications," *MRS Symp. Proc.*, **377**, 767 (1995).
8. J. I. Pankove, *Semiconductors and Semimetals, Vol. 21, Part B*, p. **245**, Academic Press, Orlando (1984).
9. R. H. Bube, *Photoconductivity of Solids*, p. 9, John Wiley & Sons, New York (1960)
10. Rose, *Concepts in Photoconductivity and Allied Problems*, p. 4, Interscience Publishers, New York (1963)
11. F. A. Rubinelli, J. Y. Hou and S. J. Fonash, "Bias-Voltage- and Bias-Light-Dependent High Photocurrent Gains in Amorphous Silicon Schottky Barriers," *J. Appl. Phys.*, **73**, 2548 (1993)
12. R. Vanderhaghen, R. Amokrane, D. Han and M. Silver, "Effect of Light-Induced Degradation on Photoconductive Gain in a-Si:H n-i-p devices," *J. Non-Cryst. Solids*, **164-166**, 599 (1993)